

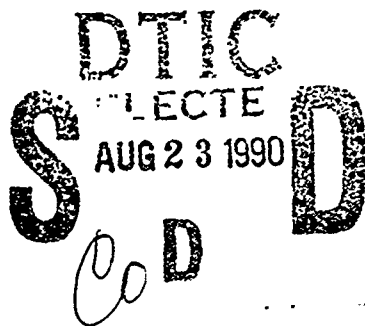
2

A Gaussian Algorithm Using Coordinate Rotation for Area Navigation
Operations with the Microwave Landing System

By

J. W. Hall
P. M. Hatzis
F. D. Powell

June 1990



AD-A225 642

Prepared for
Program Director for
Airspace Management Systems Program Office
Electronic Systems Division
Air Force Systems Command
United States Air Force
Hanscom Air Force Base, Massachusetts



Approved for public release;
distribution unlimited.

Project No. 5420

Prepared by

The MITRE Corporation
Bedford, Massachusetts

Contract No. F19628-89-C-0001

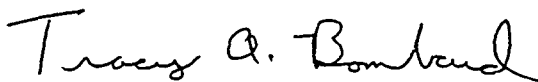
90 08 22 047

When U.S. Government drawings, specifications or other data are used for any purpose other than a definitely related government procurement operation, the government thereby incurs no responsibility nor any obligation whatsoever; and the fact that the government may have formulated, furnished, or in any way supplied the said drawings, specifications, or other data is not to be regarded by implication or otherwise as in any manner licensing the holder or any other person or conveying any rights or permission to manufacture, use, or sell any patented invention that may in any way be related thereto.

Do not return this copy. Retain or destroy.

REVIEW AND APPROVAL

This technical report has been reviewed and is approved for publication.



TRACY BOMBARD, 1LT, USAF
MMLSA Program Manager



DAVE KENYON, GM-14
MLS Division Chief

FOR THE COMMANDER



DAVID A. HERRELKO, COL, USAF
Program Director
Airspace Management Systems Program Office

UNCLASSIFIED

SECURITY CLASSIFICATION OF THIS PAGE

REPORT DOCUMENTATION PAGE

1a. REPORT SECURITY CLASSIFICATION Unclassified			1b. RESTRICTIVE MARKINGS		
2a. SECURITY CLASSIFICATION AUTHORITY			3. DISTRIBUTION/AVAILABILITY OF REPORT Approved for public release; distribution unlimited.		
2b. DECLASSIFICATION/DOWNGRADING SCHEDULE					
4. PERFORMING ORGANIZATION REPORT NUMBER(S) MTR-10765 ESD-TR-90-315			5. MONITORING ORGANIZATION REPORT NUMBER(S)		
6a. NAME OF PERFORMING ORGANIZATION The MITRE Corporation		6b. OFFICE SYMBOL (if applicable)	7a. NAME OF MONITORING ORGANIZATION		
6c. ADDRESS (City, State, and ZIP Code) Burlington Road Bedford, MA 01730			7b. ADDRESS (City, State, and ZIP Code)		
8a. NAME OF FUNDING/SPONSORING ORGANIZATION Program Director (continued)		8b. OFFICE SYMBOL (if applicable) ESD/TGM	9. PROCUREMENT INSTRUMENT IDENTIFICATION NUMBER F19628-89-C-0001		
8c. ADDRESS (City, State, and ZIP Code) Electronic Systems Division, AFSC Hanscom AFB, MA 01731-5000			10. SOURCE OF FUNDING NUMBERS PROGRAM ELEMENT NO. PROJECT NO. TASK NO. WORK UNIT ACCESSION NO. 5420		
11. TITLE (Include Security Classification) A Gaussian Algorithm Using Coordinate Rotation for Area Navigation Operations with the Microwave Landing System					
12. PERSONAL AUTHOR(S) Hall, John W., Hatzis, Patricia M., Powell, Frederic D.					
13a. TYPE OF REPORT Final		13b. TIME COVERED FROM TO		14. DATE OF REPORT (Year, Month, Day) 1990 June	
				15. PAGE COUNT 51	
16. SUPPLEMENTARY NOTATION					
17. COSATI CODES FIELD GROUP SUB-GROUP			18. SUBJECT TERMS (Continue on reverse if necessary and identify by block number) Computed Centerline Approach, Position Reconstruction Gauss-Seidel, Algorithm Microwave Landing System (MLS) Rotated Gauss-Seidel		
19. ABSTRACT (Continue on reverse if necessary and identify by block number) The Microwave Landing System (MLS) avionics convert the received signals of range, azimuth angle, and elevation angle to yield aircraft position in Cartesian coordinates. This enables area navigation and computed centerline approaches, including multi-leg and curved approaches. When the three MLS ground units are not collocated, this requires iteration. The speed of convergence and the size of the algorithm and its computational burden affect the MLS avionics storage and timing requirements. Gaussian algorithms tend to be relatively compact but diverge at azimuth angles within the coverage of the MLS, while Newton-Raphson algorithms require more storage and impose a greater computational burden. This report presents a Gaussian algorithm which, by rotating the coordinate system, enables fast convergence everywhere within the MLS coverage, and with a computational burden significantly less than an equivalent Newton-Raphson algorithm.					
20. DISTRIBUTION/AVAILABILITY OF ABSTRACT <input type="checkbox"/> UNCLASSIFIED/UNLIMITED <input checked="" type="checkbox"/> SAME AS RPT. <input type="checkbox"/> DTIC USERS			21. ABSTRACT SECURITY CLASSIFICATION Unclassified		
22a. NAME OF RESPONSIBLE INDIVIDUAL Judith P. Schultz			22b. TELEPHONE (Include Area Code) (617) 271-8087		22c. OFFICE SYMBOL Mail Stop D135

DD FORM 1473, 84 MAR

83 APR edition may be used until exhausted.
All other editions are obsolete.

SECURITY CLASSIFICATION OF THIS PAGE

UNCLASSIFIED

UNCLASSIFIED

8a. for Airspace Management Systems Program Office

UNCLASSIFIED

EXECUTIVE SUMMARY

The Microwave Landing System not only enables precision low approach and landing, it also supports area navigation. This enables multi-leg, curved, and computed-centerline approaches. These procedures require the avionics to determine the aircraft location anywhere within the region of coverage, which may at some airports be as large as $\pm 60^\circ$ in azimuth and 30° in elevation. This process requires reconstructing the aircraft position in Cartesian coordinates, given the ground units' site data and the observations of azimuth and elevation angles, and distance from a distance measuring equipment. When the ground units are not collocated, iteration is required.

Position reconstruction algorithms based on Gaussian techniques converge very slowly, or diverge, for some geometries of ground unit and aircraft location which are within the system coverage. On the other hand, algorithms based on Newton-Raphson techniques usually converge very rapidly but impose a significantly greater storage requirement and computational burden on the avionics. This report presents a modified Gaussian algorithm which uses coordinate system rotation to achieve rapid convergence for all geometries, and with a computational burden much less than the equivalent Newton-Raphson algorithm. It presents the theoretical foundations of this algorithm and various results showing its effects, and compares its storage and computational burdens against Gaussian and Newton-Raphson equivalents in the MLS context.

Accession For	
NTIS CRA&I	<input checked="" type="checkbox"/>
DTIC TAB	<input type="checkbox"/>
Unannounced	<input type="checkbox"/>
Justification	
By _____	
Distribution /	
Availability codes	
Dist	Avail and/or Special
A-1	



ACKNOWLEDGMENT

This document has been prepared by The MITRE Corporation under Project No. 5420, Contract No. F19628-89-C-0001. The contract is sponsored by the Electronic Systems Division, Air Force Systems Command, Hanscom Air Force Base, Massachusetts 01731-5000.

TABLE OF CONTENTS

SECTION	PAGE
1 Introduction	1
2 Principles of Gauss-Seidel Iteration	3
3 Geometry, Notation and Mathematics	5
4 An Irrotational Gauss-Seidel MLS Algorithm	7
4.1 Definition	7
4.2 Performance	7
4.3 Analysis	9
5 A Rotational Gauss-Seidel MLS Algorithm	13
5.1 Definition	13
5.2 Performance	17
5.3 Analysis	19
6 Comparisons of Performance	23
List of References	25
Appendix A FORTRAN 77 Computer Code	27
Appendix B Alternate Newton-Raphson Algorithm	29
Appendix C The Sine Form of the RGSi	31
Appendix D Exercise of the Rotational Algorithm	33

LIST OF FIGURES

FIGURE	PAGE
2-1 Fast Convergence	3
2-2 Slow Convergence	3
2-3 The Rotation Principle	4
3-1 Geometry	6
5-1 Conical and Planar Azimuth Angles	14
A-1 Computer Code	27

LIST OF TABLES

TABLE	PAGE
4-1 Divergence with a GSI PRA	8
4-2 Slow Convergence with a GSI PRA	8
5-1 RGSi in Table 4-1 Case	17
5-2 RGSi in Table 4-2 Case	18
5-3 Behavior of the RGSi PRA with a Large Azimuth Angle	18
6-1 Comparison of Various PRAs	23
D-1 Rotational Algorithm Exercise	34

SECTION 1

INTRODUCTION

The international civil aviation community plans to replace the Instrument Landing System by the Microwave Landing System (MLS) [1] during the next decade. Among the reasons are that the MLS enables much more precise determination of the aircraft's location, and has much wider coverage. These added capabilities will enable conduct of area navigation (RNAV), including curved approaches, in the vicinity of the airport. Further, it will not be necessary to locate the MLS azimuth antenna on the runway centerline; offset sites and therefore offset runways can be used, or the same set of ground units can service several runways. These new capabilities are accompanied by new complexities.

In RNAV, or computed centerline, operation with the MLS, it is necessary, given the data which define the sites of the three ground units, and the observations of azimuth angle, elevation angle, and distance measuring equipment (DME), to determine in the avionics the aircraft position in Cartesian coordinates relative to the centerline of the desired runway. This process is not simple when the ground units are not collocated, and iteration is required to reconstruct the aircraft position from the data and observations. Two general types, or classes, of algorithms have been suggested [2], for this purpose, Gaussian and Newton-Raphson. Gaussian position reconstruction algorithms (PRAs) are attractive as they tend to have small storage and computational burdens, in comparison to Newton-Raphson PRAs. However, they also tend to have problems of divergence or slow convergence, depending on the particular algorithm and the geometry of the situation, for azimuth angles which are within the system's lateral coverage of $\pm 60^\circ$. On the other hand, Newton-Raphson PRAs may have singularities that preclude use in various regions of the MLS coverage. This paper presents a modified Gaussian PRA which has no singularities and which, by using rotations, conditions the problem so that iteration is stable and rapid everywhere within the MLS coverage. This algorithm holds a position intermediate between Gaussian and Newton-Raphson methods. It is slightly less compact than the equivalent Gaussian algorithm, and has a greater computational burden; however, it converges faster and converges everywhere. The algorithm converges more slowly than the equivalent Newton-Raphson PRA; however, it is more compact, has no singularities, and has a significantly-reduced computational burden.

Section 2 presents a heuristic discussion of the principles of the fastest member of the class of Gaussian algorithms, Gauss-Seidel iteration (GSI), in a simple and general way to show the operating principles of the GSI process, and especially to motivate the concept of coordinate rotation in this application. Section 3 provides the notation and mathematical

foundation, section 4 develops and shows the behavior of a conventional irrotational GSI MLS PRA, and section 5 extends section 4 to include the rotation principle and thus form a rotational Gauss-Seidel iterative (RGSI) PRA. Comparisons of speed, computational burden, and storage requirements against both a GSI and a Newton-Raphson PRA are presented in section 6, followed by conclusions. Appendixes give the computer code for the proposed algorithm, the formulation of the Newton-Raphson PRA which was used for comparisons, analysis of an alternate formulation for the RGSI PRA, and a small but representative sample of the behavior of this algorithm for a variety of ground unit geometries and aircraft location.

SECTION 2

PRINCIPLES OF GAUSS-SEIDEL ITERATION

This section presents a heuristic discussion of the principles of Gauss-Seidel iteration (GSI). Its purposes are to provide an intuitive, although rudimentary, understanding of GSI, and, especially, to motivate the application of the rotation principle used in this study.

Consider a pair of nonlinear functions, f and g , of x and y . The functions are continuous in the vicinity of their unique solution, and it is assumed that the magnitude of the slope of f with respect to x is small compared to that of g . This situation is shown in figure 2-1. An initial condition, x_0 , is assumed for x , and f is evaluated with this value, yielding y_1 . The other equation, g , is then evaluated with y_1 , yielding x_1 which is in turn used in f to find y_2 , etc. As iteration continues, the successive estimates of x and y converge to the solution. The process is shown by arrows in the figure.

Now consider the effect if the slope of f is appreciably greater, as in figure 2-2. It is evident that the process converges much more slowly than in figure 2-1.

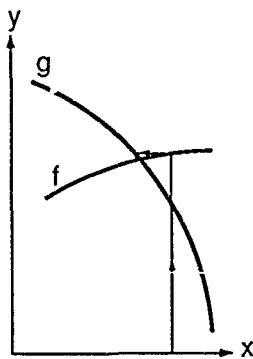


Figure 2-1. Fast Convergence

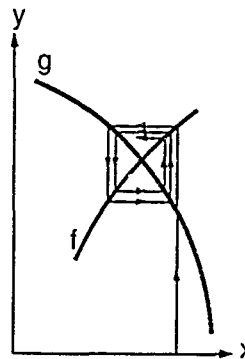


Figure 2-2. Slow Convergence

Some of the principles of GSI may be deduced from these figures:

- The increments to x and y are parallel to the x and y axes;
- Convergence slows as the magnitude of the slope of f increases;
- New values of x and y are used as soon as they are available.

If convergence is too slow, it would presumably help if the increments were not constrained to be parallel to the x and y axes. In particular, it would be especially helpful if the increments could be parallel to the slope of the function f , as with Newton methods. This can be accomplished by using a rotated set of coordinates, x^* and y^* , such that (x^*) is parallel to f at each iteration-point. In this situation, shown in figure 2-3, the slope of f with respect to x^* is almost zero at each iteration, each increment is in the x^* direction, rather than the x direction, and thus the iteration, with each Δx^* step, will go almost directly to the solution-point. This is the motivation for exploring the utility of rotation as a conditioning method for rectifying an ill-conditioned problem.

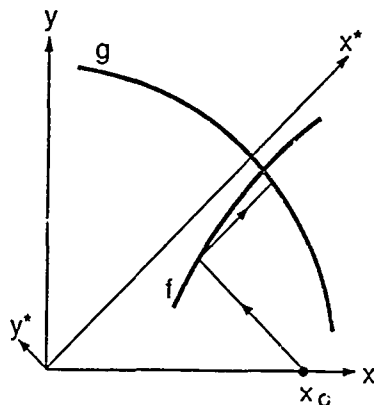


Figure 2-3. The Rotation Principle

The analogy between the very simple example outlined above and the MLS problem is now presented. The function f is, at least to some extent, similar to the azimuth-angle guidance locus, while the function g is similar to the DME locus. The idea of using rotations as a means to improve convergence speed and stability is especially attractive since the required rotation angle is approximately the observed azimuth angle, and is thus provided a priori as an input to the PRA.

These ideas will now be more formally developed.

SECTION 3

GEOMETRY, NOTATION AND MATHEMATICS

This section presents the geometry, notation, and the mathematical foundations for the MLS PRA problem.

The coordinate system for the problem is defined in figure 3-1. The MLS x-axis is selected to be the runway centerline and its extension, with negative values toward the stop-end of the runway. The origin of the coordinate system is set at the runway threshold so that a conventional location for the ground equipment has a negative x-value. Thus, an azimuth antenna located near the stop-end of a 5000 foot runway has an x-value of approximately $x_A = -5000$, where the subscript A implies azimuth antenna. The positive direction of y lies to the left of an observer who is standing at the origin with the stop-end of the runway behind him. The positive direction of z is up. The elevation angle is defined as positive counterclockwise looking along the positive y-axis so that positive angles correspond to positive altitude. Azimuth is defined as positive clockwise from the x-axis, looking down towards the ground. This coordinate system is not right-handed but conforms to that of [1] and [2]. The azimuth antenna boresight is assumed, for simplicity but without loss of generality, to be parallel to the runway centerline; a well-known rotation and de-rotation enable treating other orientations.

The ground units' site data, defined below, are transmitted to the aircraft.

x_A, y_A, z_A	Components of location of azimuth antenna
x_D, y_D, z_D	Components of position of DME
x_E, y_E, z_E	Components of position of elevation antenna
x_T, y_T, z_T	Components of true position of the aircraft
x_i, y_i, z_i	Components of the i^{th} estimate, $i=0, 1, 2, \dots$
θ, ϕ	Observed conical azimuth and elevation angles
ρ	Observed slant range from the DME
P, C	Subscripts: planar (P), conical (C)

The observations received in the aircraft, ρ , ϕ and θ , are generated respectively by a distance-measuring equipment (DME), a conical-pattern

azimuth antenna (AZ), and a conical-pattern elevation antenna (EL).

Figure 3-1 shows a typical and general geometrical situation.

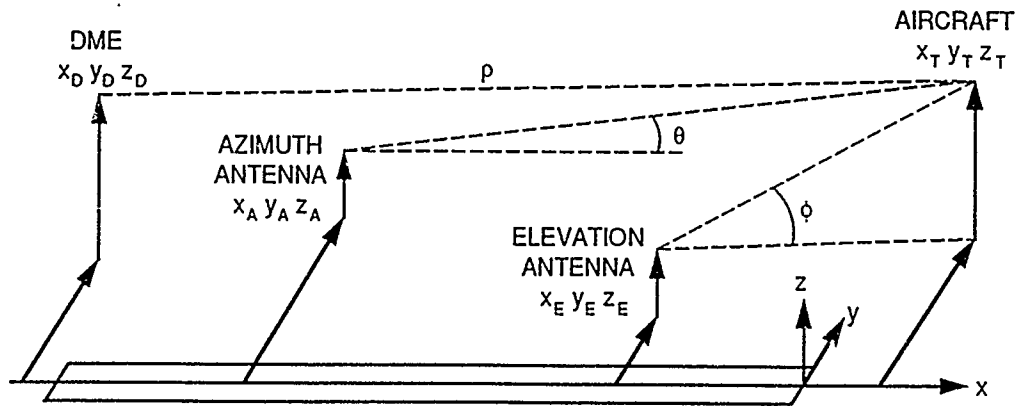


Figure 3-1. Geometry

The observations in the aircraft are now defined.

The observed slant range from the DME to the aircraft is ρ , where

$$\rho = [(x_T - x_D)^2 + (y_T - y_D)^2 + (z_T - z_D)^2]^{1/2} \quad (3-1)$$

The azimuth antenna forms a conical beam, with the axis of radial symmetry parallel to the y-axis. The observed azimuth angle at the aircraft is θ_C , measured exterior to the cone, where

$$\tan \theta_C = -(y_T - y_A) / [(x_T - x_A)^2 + (z_T - z_A)^2]^{1/2} \quad (3-2)$$

Similarly, the elevation antenna forms an always-conical beam, with a vertical axis of radial symmetry. The observed elevation angle at the aircraft is ϕ , measured exterior to the cone, where

$$\tan \phi = (z - z_E) / [(x - x_E)^2 + (y - y_E)^2]^{1/2} \quad (3-3)$$

The geometrical site data and the observations are combined in the avionics' PRA to determine the aircraft's location.

SECTION 4

AN IRROTATIONAL MLS GAUSS-SEIDEL ALGORITHM

A typical irrotational GSI MLS PRA is now formed. It will be used as the basis for a rotational algorithm (RGSI), and will also enable comparisons of performance and complexity. Three distinct topics are addressed in this section:

- a. An irrotational Gaussian PRA will be defined;
- b. It will be shown that this PRA can diverge or converge slowly within the MLS RNAV coverage;
- c. The properties of this PRA will be demonstrated analytically.

4.1 DEFINITION

The observations, ρ , ϕ , and θ lead to a GSI PRA which is, in essence, identical to Case 9 of [2] and [4]. Initial conditions for x_0 and y_0 are required, but an initial condition for z_0 is not needed.

Conical elevation equation (3-3) solved for altitude, z

$$z_{i+1} = z_E + [(x_i - x_E)^2 + (y_i - y_E)^2]^{1/2} \tan \phi \quad (4-1)$$

Conical azimuth equation (3-2) solved for lateral position, y

$$y_{i+1} = y_A - [(x_i - x_A)^2 + (z_{i+1} - z_A)^2]^{1/2} \tan \theta_C \quad (4-2)$$

DME equation (3-1) solved for along-runway position, x

$$x_{i+1} = x_D + [\rho^2 - (z_{i+1} - z_D)^2 - (y_{i+1} - y_D)^2]^{1/2} \quad (4-3)$$

Iterate to (4-1) until a solution of acceptable accuracy is reached.

4.2 PERFORMANCE

Table 4-1 shows that this PRA can diverge. The four lines at the top of the table show the geometry of the three ground units; the azimuth antenna is in a conventional split-site arrangement, but the DME is collocated with the elevation unit, in accordance with a suggestion in [5]. Below this area is a line which presents the observations; notice that the observed azimuth angle is 37.95° , less than the minimum MLS coverage of 40° . The four lines below that are organized in columns: the first column shows the three components of the aircraft's true location, the second

shows the initial condition assumption, and the other six columns show the estimated position after each of six iterations; the iteration number heads the column. In column 2, the place for z_0 is blank, as that initial condition is not needed. The process is divergent: at each stage the estimates of x and y are further from the true location, although z converges. The initial conditions were arbitrarily selected to show the divergence clearly, and are thus not consistent with the initialization proposed in [2]. The configuration in this figure is 3-9 (ground unit arrangement 3, and aircraft location 9), consistent with the database of exercises; this nomenclature appears in the heading of ground geometry and aircraft position in the table.

Table 4-1. Divergence with a GSI PRA

GROUND STATION SITE GEOMETRY # 3								
AZIMUTH ANTENNA SITE			DME TRANSMITTER SITE			ELEVATION ANTENNA SITE		
X	Y	Z	X	Y	Z	X	Y	Z
-6000.	-1000.	10.	-1000.	500.	5.	-1000.	500.	5.
AIRCRAFT POSITION #9. OBSERVED DATA: RHO=12588.3 THETA=37.95 PHI=16.12								
TRUE POS.		INIT. POS.						
ITERATION NUMBER I	1	2	3	4	5	6		
X	5000.00	5500.00	4061.68	6092.74	3264.82	6824.62	1337.77	8210.56
Y	-10000.00	-10500.00	-10418.31	-9301.11	-10815.98	-8720.97	-11365.27	-7336.81
Z	3500.00		3697.55	3482.99	3501.42	3499.88	3500.01	3500.00

Table 4-2. Slow Convergence with a GSI PRA

GROUND STATION SITE GEOMETRY # 2								
AZIMUTH ANTENNA SITE			DME TRANSMITTER SITE			ELEVATION ANTENNA SITE		
X	Y	Z	X	Y	Z	X	Y	Z
-6000.	0.	5.	-6000.	0.	5.	-1000.	500.	5.
AIRCRAFT POSITION #29. OBSERVED DATA: RHO=36976.0 THETA=32.74 PHI=4.31								
TRUE POS.		INIT. POS.						
ITERATION NUMBER I	1	2	3	4	5	6		
X	25000.00	31100.24	22041.99	26139.90	24517.92	25196.47	24918.69	25033.45
Y	-20000.00	-20000.00	-23929.78	-18106.58	-20730.01	-19691.33	-20125.80	-19947.93
Z	2500.00		2875.13	2535.59	2484.62	2506.40	2497.38	2501.08

Table 4-2, (configuration 2-29), organized in the same format, shows an example of slow convergence with this algorithm. The ground units are arranged in a conventional split-site; the DME is collocated with the azimuth unit. The initialization uses the procedure suggested in [2]. But after five iterations, the error in lateral position is -125.80'. This error is excessive according to the criterion for slow convergence and excessive error set forth below.

An allowance of 0.017° is given in [1] for the "Path Following Error" which may be tolerated in the avionics. There are many sources of error in the avionics; some are governed by physical considerations such as received signal power which impose limits on performance. But, in principle, the algorithm can yield an almost-perfect result. The algorithm, for this discussion, is therefore allowed an error of $0.017^\circ/3$, which is negligible when added RSS; this allowance is approximately 0.01%, and the value $(x_T/10,000)$ is used hereafter. The algorithm is considered to be slow if the magnitude of the error in any variable exceeds $(x_T/10,000)$ after five iterations.

The examples shown in these tables are not exceptional; they are intended to show that an irrotational GSI may have unsatisfactory behavior in geometrical situations which might be expected in MLS RNAV.

4.3 ANALYSIS

A rigorous analysis of the stability and speed of convergence of a Gauss-Seidel MLS algorithm is now developed, following [3].

The procedure is outlined:

- (a) The method of analysis for GSI algorithms assumes that the functions are linear; therefore (4-1) through (4-3) are linearized about the solution at x_T , y_T , z_T ;
- (b) Two matrices are formed: A matrix S is the coefficient of the $(i+1)$ values of the variables, while a matrix T is the coefficient of the (i) values of the variables;
- (c) The eigenvalues of the matrix-product $(S^{-1}T)$ are determined. These are the values of λ for which the determinant $\Delta = |I\lambda - S^{-1}T|$ is zero, where I is the identity matrix in three variables.

The error at each iteration changes by the factor λ' , where that is the eigenvalue of greatest magnitude. If $\lambda' < 0$, the error oscillates at each iteration; if $|\lambda'| = 1$, the iteration will not converge, while if $|\lambda'| > 1$ the iteration diverges.

Following the procedure outlined above, expand the three functions by a multi-dimensional Taylor series about the solution at x_T, y_T, z_T ; the linearized increments about the solution-point are

$$\Delta z_{i+1} = [(x_T - x_E) \tan \phi / R_E] \Delta x_i + [(y_T - y_E) \tan \phi / R_E] \Delta y_i \quad (4-4)$$

$$\Delta y_{i+1} = -[(x_T - x_A) \tan \theta / R_A] \Delta x_i - [(z_T - z_A) \tan \theta / R_A] \Delta z_{i+1} \quad (4-5)$$

$$\Delta x_{i+1} = -[(y_T - y_D) / R_D] \Delta y_{i+1} - [(z_T - z_D) / R_D] \Delta z_{i+1} \quad (4-6)$$

where

$$R_E = [(x_T - x_E)^2 + (y_T - y_E)^2]^{1/2} \quad (4-7)$$

$$R_A = [(x_T - x_A)^2 + (z_T - z_A)^2]^{1/2} \quad (4-8)$$

$$R_D = [\rho^2 - (y_T - y_D)^2 - (z_T - z_D)^2]^{1/2} \quad (4-9)$$

Then, following step (b), the matrix of the (i+1) coefficients is S, where the first row is from (4-6), the second is from (4-5), while the third row is from (4-4). The vector of variables which post-multiplies S is $(\Delta x_{i+1}, \Delta y_{i+1}, \Delta z_{i+1})^T$, so that

$$S = \begin{pmatrix} 1 & [(y_T - y_D) / R_D] & [(z_T - z_D) / R_D] \\ 0 & 1 & [(z_T - z_A) \tan \theta / R_A] \\ 0 & 0 & 1 \end{pmatrix} \quad (4-10)$$

and the matrix of the (i) coefficients is T, in the same order.

$$T = \begin{pmatrix} 0 & 0 & 0 \\ -[(x_T - x_A) \tan \theta / R_A] & 0 & 0 \\ [(x_T - x_E) \tan \phi / R_E] & [(y_T - y_E) \tan \phi / R_E] & 0 \end{pmatrix} \quad (4-11)$$

The matrix S^{-1} is easily written directly from (4-10), as

$$S^{-1} = \begin{pmatrix} 1 & -s_{12} & (s_{12}s_{23} - s_{13}) \\ 0 & 1 & -s_{23} \\ 0 & 0 & 1 \end{pmatrix} \quad (4-12)$$

and $\Delta = |I_3 \lambda - S^{-1} T|$ is

$$\Delta = \begin{vmatrix} \lambda - [-s_{12}t_{21} + t_{31}(s_{12}s_{23} - s_{13})] & -[t_{32}(s_{12}s_{23} - s_{13})] & 0 \\ -[t_{21} - s_{23}t_{31}] & \lambda + [s_{23}t_{32}] & 0 \\ -t_{31} & -t_{32} & \lambda \end{vmatrix} \quad (4-13)$$

Expanding (4-13) by minors of the third column yields

$$\Delta = \lambda \{ \lambda^2 + \lambda [s_{23}t_{32} + s_{12}t_{21} - t_{31}(s_{12}s_{23} - s_{13})] + s_{13}t_{21}t_{32} \} = 0 \quad (4-14)$$

The term within the braces of (4-14) is in the form $\{\lambda^2 + B\lambda + C\}$, where

$$B = [(z_T - z_A) \tan \theta \tan \phi / R_A] \{ [(y_T - y_E) / R_E] - [(x_T - x_E) / R_E] [(y_T - y_D) / R_D] \} \\ - [(y_T - y_D) / R_D] [(x_T - x_A) / R_A] \tan \theta + [(x_T - x_E) / R_E] [(z_T - z_D) / R_D] \tan \phi$$

and

$$C = -[(x_T - x_A) / R_A] [(y_T - y_E) / R_E] [(z_T - z_D) / R_D] \tan \theta \tan \phi \quad (4-15)$$

$$(4-16)$$

A simplification is useful in order to enable physical interpretation of this result. Assume a configuration with the three ground units collocated at the origin; then $x_D = y_D = z_D = 0$, $x_A = y_A = z_A = 0$, and $x_E = y_E = z_E = 0$. As a result, $z_T / R_E = \tan \phi$, $y_T / R_A = -\tan \theta$, and $R_D = x_T$. This set of assumed values reduces (4-15) and (4-16) to $B = \tan^2 \theta + \tan^2 \phi$ and $C = \tan^2 \theta \tan^2 \phi$, and the determinant becomes

$$\Delta = \lambda [\lambda^2 + (\tan^2 \theta + \tan^2 \phi) \lambda + \tan^2 \theta \tan^2 \phi] = \lambda (\lambda + \tan^2 \theta) (\lambda + \tan^2 \phi) \quad (4-17)$$

with solutions

$$\lambda = 0, \lambda = -\tan^2 \theta, \text{ and } \lambda = -\tan^2 \phi. \quad (4-18)$$

The iteration becomes unstable if either angle exceeds 45 degrees. Elevation angles above 30 degrees are out of coverage, but, as noted above, the azimuth angle may be large enough to cause divergence.

SECTION 5

A ROTATIONAL GAUSS-SEIDEL MLS ALGORITHM

The irrotational GSI presented in section 4 is now used as the basis for developing the rotational GSI (RGSI) in this section. This section has three parts, in which the topics of definition of the RGSI, its performance, and its analysis are presented.

5.1 DEFINITION

The irrotational GSI presented above is now used as the basis for development of the RGSI; it was defined in section 4 by the relationships

Conical elevation equation (3-3) solved for altitude, z

$$z_{i+1} = z_E + [(x_i - x_E)^2 + (y_i - y_E)^2]^{1/2} \tan \phi \quad (5-1)$$

Conical azimuth equation (3-2) solved for lateral position, y

$$y_{i+1} = y_A - [(x_i - x_A)^2 + (z_{i+1} - z_A)^2]^{1/2} \tan \theta_C \quad (5-2)$$

DME equation (3-1) solved for along-runway position, x

$$x_{i+1} = x_D + [\rho^2 - (z_{i+1} - z_D)^2 - (y_{i+1} - y_D)^2]^{1/2} \quad (5-3)$$

Iterate to (5-1) until a solution of acceptable accuracy is reached.

The RGSI exhibits better convergence for high elevation angles, independent of azimuth, if (5-1) is replaced by

$$z_{i+1} = z_E + [(x_i - x_E)^2 + (y_i - y_E)^2 + (z_i - z_E)^2]^{1/2} \sin \phi \quad (5-4)$$

which may be derived from (5-1) or the geometry. This formulation is used to generate the numerical results. However, the prior formulation (5-1) is used in this section to maintain symmetry with the GSI and its analysis.

The geometry of a conical azimuth antenna system, figure 5-1, shows that the horizontal plane projection of the observed conical azimuth angle points to the horizontal projection of the aircraft location only when the aircraft altitude is zero. Therefore, the ideal rotation places the rotated x^* -axis so that it passes through that projection. This step brings the new x^* axis parallel to the planar azimuth angle, which is independent of altitude, rather than the conical azimuth, which is a function of the altitude, as in figure 2-1. But the relationship between the planar and conical azimuth angles must involve the altitude, as shown in figure 5-1.

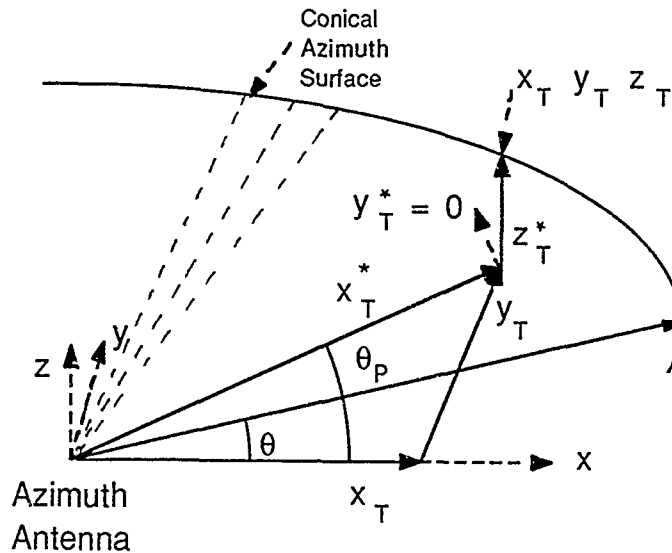


Figure 5-1. Conical and Planar Azimuth Angles

The rotation shown in figure 5-1 requires that the coordinate origin be moved to the azimuth site prior to the rotation, as in (5-5).

Aircraft	$x_i' = x_i - x_A$	$y_i' = y_i - y_A$	$z_i' = z_i - z_A$
Azimuth	$x_A' = x_A - x_A = 0$	$y_A' = y_A - y_A = 0$	$z_A' = z_A - z_A = 0$
DME	$x_D' = x_D - x_A$	$y_D' = y_D - y_A$	$z_D' = z_D - z_A$
Elevation	$x_E' = x_E - x_A$	$y_E' = y_E - y_A$	$z_E' = z_E - z_A$

(5-5)

where the primes (') imply translated variables. It is not necessary to translate nor rotate the z-components, but some reduction of the required computations during the iteration, and a more orderly notation, result if they are translated.

The desired rotation of coordinates about the newly translated origin of figure 5-1 is defined by the matrix equation

$$\begin{pmatrix} x^* & x_A^* & x_D^* & x_E^* \\ y^* & y_A^* & y_D^* & y_E^* \\ z^* & z_A^* & z_D^* & z_E^* \end{pmatrix} = \begin{pmatrix} \cos\theta_P & -\sin\theta_P & 0 \\ \sin\theta_P & \cos\theta_P & 0 \\ 0 & 0 & 1 \end{pmatrix} \begin{pmatrix} x' & x_A' & x_D' & x_E' \\ y' & y_A' & y_D' & y_E' \\ z' & z_A' & z_D' & z_E' \end{pmatrix} \quad (5-6)$$

where the superscript stars (*) imply both translation and rotation, and the subscripts (i) have been omitted as redundant. As (5-5) sets the offsets $x_A' = y_A' = z_A' = 0$, then $x_A^* = y_A^* = z_A^* = 0$ in (5-6) and may be omitted. This rotation causes the horizontal-plane projection of the lateral position y^* of the aircraft in the rotated coordinates to converge to zero.

of (5-6) expresses the fact that, as the rotation is the horizontal plane, about the z-axis, the z-values are not rotated.

However, the required rotation angle is the planar azimuth angle, θ_p . This angle is not available as an observation, but must be deduced from the observation of the conical angle, θ_c .

From (5-4), the conical azimuth angle is

$$\sin\theta_c = -(y-y_A)/[(x-x_A)^2+(y-y_A)^2+(z-z_A)^2]^{1/2}$$

When evaluated at $z = z_A$ this reduces to the planar azimuth angle

$$\sin\theta_p = -(y-y_A)/[(x-x_A)^2+(y-y_A)^2]^{1/2}$$

so that the quotient of these two expressions yields the relationship

$$\sin\theta_p = \{1+(z-z_A)^2/[(x-x_A)^2+(y-y_A)^2]\}^{1/2}\sin\theta_c \quad (5-7)$$

Now, (5-7) may be used to calculate θ_p exactly only when the values of x, y, and z are the exactly correct values. Otherwise, the right hand side values for x, y, and z are the estimated aircraft location at the end of any iteration cycle, and the left hand side is the estimated value of the planar azimuth angle. However, as the process converges, at each iteration it yields a better set of values for estimated position. It thus also yields a better estimate of $\sin\theta_p$, and therefore converges towards the exactly correct location of the aircraft. Note that (5-7) reduces to $\sin\theta_p = \sec\phi\sin\theta_c$ if the elevation and azimuth antennas are collocated.

The iterative process now takes the form:

Translated and rotated elevation equation solved for altitude, z^* ,

$$z_{i+1}^* = z_E^* + [(x_i^*-x_E^*)^2+(y_i^*-y_E^*)^2]^{1/2} \tan\phi \quad (5-8)$$

This may be simplified, for y_i^* may be set to zero as that is the terminal result known a priori.

The translated and rotated lateral position estimate equation vanishes, for the correct rotation, θ_p , is that for which $y^* = 0$. As the iteration proceeds, the estimate of $\sin\theta_p$ converges to the correct value thereof, and since the translation (5-5) forced y_A^* to be zero, then y_i^* converges to zero. This equation therefore becomes identically zero and may be omitted. Omission does not reduce the complexity of the problem, for the y^* equation is replaced by the required rotation-equation.

Translated and rotated DME equation solved for position, x^*

$$x_{i+1}^* = x_D^* + [\rho^2 - (y_{i+1}^* - y_D^*)^2 - (z_{i+1}^* - z_D^*)^2]^{1/2} \quad (5-9)$$

in which, again, $y^* = 0$ may be used.

Translated and rotated coordinate value of the estimated sine of the planar azimuth angle required for the coordinate rotation

$$\hat{\sin\theta_{pi+1}} = [1 + (z_{i+1}^*/x_{i+1}^*)^2]^{1/2} \sin\theta_C \quad (5-10)$$

from (5-7), where the hat ($\hat{}$) shows that ($\sin\theta_p$) is estimated, not (θ_p). Again, $y^* = 0$ has been used as the a priori knowledge of the final result of the iteration, and x_A^* , y_A^* and z_A^* have been omitted, as before, since the translation step forced them to be identically zero. The estimated cosine of the planar azimuth angle required for the rotation of coordinates is calculated directly from (5-10) using a trigonometrical identity. An equivalent to (5-10) can be reached by using $\tan\theta_p$ and $\tan\theta_C$ functions, instead of the sines.

The process is now iterated, returning to (5-6) and (5-8).

When the solution has stabilized, the de-rotation and de-translation are performed in that order to find the aircraft location in the original coordinates. The de-rotation uses the inverse of (5-6) with the calculated planar azimuth angle to find x' and y' , and the de-translation uses the inverse of (5-5) to find x and y . The inverse rotation, with fewer variables than the direct rotation, is

$$\begin{pmatrix} x' \\ y' \\ z' \end{pmatrix} = \begin{pmatrix} \cos\theta_p & \sin\theta_p & 0 \\ -\sin\theta_p & \cos\theta_p & 0 \\ 0 & 0 & 1 \end{pmatrix} \begin{pmatrix} x^* \\ y^* \\ z^* \end{pmatrix}$$

As $y^* = 0$, this can be simplified to

$$\begin{pmatrix} x' \\ y' \\ z' \end{pmatrix} = \begin{pmatrix} \cos\theta_p & 0 \\ -\sin\theta_p & 0 \\ 0 & 1 \end{pmatrix} \begin{pmatrix} x^* \\ z^* \end{pmatrix} \quad (5-11)$$

The inverse translation is

$$\begin{aligned} x &= x' + x_A \\ y &= y' + y_A \\ z &= z' + z_A \end{aligned} \quad (5-12)$$

This completes definition of the rotational algorithm. As was noted above, this is somewhat more complex than the basic GSI, for although the rotation-angle equation (5-10) replaced the lateral-displacement equation, the rotation process (5-6) must be repeated at each iteration. The steps

of de-rotation (5-11) and de-translation (5-12) impose additional storage and computation burdens, although they are outside the iteration. Nonetheless, the improved speed, and, especially, the universal stability of the rotational algorithm will be shown to justify these additions.

5.2 PERFORMANCE

The performance of the RGSI is now discussed.

In section 4, tables 4-1 and 4-2 showed that the GSI may diverge or be slow to converge within the coverage of the MLS. Tables 5-1 and 5-2, below, show the behavior of the RGSI for the same conditions. A variety of other cases are presented in appendix C, which contains an abbreviated sample of the exercise of this algorithm. It should be noted that, in addition to the initial conditions x_0 and y_0 used in the GSI PRA, the RGSI PRA also requires the initial condition z_0 (arbitrarily set to 3000' here).

Table 5-1. RGSI in Table 4-1 Case

GROUND STATION SITE GEOMETRY # 3								
AZIMUTH ANTENNA SITE			DME TRANSMITTER SITE			ELEVATION ANTENNA SITE		
X	Y	Z	X	Y	Z	X	Y	Z
-6000.	-1000.	10.	-1000.	500.	5.	-1000.	500.	5.
AIRCRAFT POSITION #9. OBSERVED DATA: RHO=12588.3 THETA=37.95 PHI=16.12								
TRUE POS. INIT. EST.								
ITERATION NUMBER I	1	2	3	4	5	6		
X	5000.00	5500.00	5061.23	4982.69	4998.14	5000.27	5000.04	5000.00
Y	-10000.00	-10500.00	-10071.39	-9994.98	-9998.41	-10000.04	-10000.03	-10000.00
Z	3500.00	3000.00	3608.70	3533.09	3499.11	3499.32	3499.99	3500.01

In tables 5-1 and 5-2, it is evident that there is no sign of either slow convergence nor of divergence.

Table 5-3 shows the behavior of the RGSI PRA in a case involving a large azimuth angle. The GSI PRA of section 4 was divergent for this case.

Table 5-2. RGSi in Table 4-2 Case

GROUND STATION SITE GEOMETRY # 2								
AZIMUTH ANTENNA SITE			DME TRANSMITTER SITE			ELEVATION ANTENNA SITE		
X	Y	Z	X	Y	Z	X	Y	Z
-6000.	0.	5.	-6000.	0.	5.	-1000.	500.	5.
AIRCRAFT POSITION #29. OBSERVED DATA: RHO=36976.0 THETA=32.74 PHI=4.31								
TRUE POS. INIT. EST.								
ITERATION NUMBER I	1	2	3	4	5	6		
X	25000.00	31100.24	24966.68	24999.97	25000.00	25000.00	25000.00	25000.00
Y	-20000.00	-20000.00	-20000.00	-20000.00	-20000.00	-20000.00	-20000.00	-20000.00
Z	2500.00	2778.47	2884.17	2500.38	2500.00	2500.00	2500.00	2500.00

Table 5-3. Behavior of the RGSi PRA with a Large Azimuth Angle

GROUND STATION SITE GEOMETRY # 2								
AZIMUTH ANTENNA SITE			DME TRANSMITTER SITE			ELEVATION ANTENNA SITE		
X	Y	Z	X	Y	Z	X	Y	Z
-6000.	0.	5.	-6000.	0.	5.	-1000.	500.	5.
AIRCRAFT POSITION #12. OBSERVED DATA: RHO=25631.8 THETA=-51.29 PHI=2.54								
TRUE POS. INIT. EST.								
ITERATION NUMBER I	1	2	3	4	5	6		
X	10000.00	16030.91	9988.85	9999.99	10000.00	10000.00	10000.00	10000.00
Y	20000.00	20000.00	20000.00	20000.00	20000.00	20000.00	20000.00	20000.00
Z	1000.00	1138.01	1165.55	1000.11	1000.00	1000.00	1000.00	1000.00

5.3 ANALYSIS

This subsection presents the analysis of the stability characteristics of the RGS. It follows the form of section 4.3, and uses the same mathematical procedures.

The key equations are expanded by a multi-dimensional Taylor series about the solution point. The independent variables of the expansion are the altitude estimate, the lateral-position estimate, and the estimate of the sine of the planar azimuth angle. There are several dependent variables that did not appear in the prior work; these are the partial derivatives of the ground unit locations with respect to the estimated sine of the planar azimuth angle.

The increments are formed.

From (5-8) converted to the tangent form of the altitude equation, shown in (5-1), in order to show the key difference between this RGS PRA and the irrotational PRA of section 4,

$$\Delta z_{i+1}^* = \{(x_T^* - x_E^*)[\Delta x_i^* - (\partial x_E^* / \partial q) \Delta q_i] + (y_E^*)(\partial y_E^* / \partial q) \Delta q_i\} \tan \phi / R_E \quad (5-14)$$

where

$$R_E = [(x_T^* - x_E^*)^2 + (y_E^*)^2]^{1/2} \quad (5-15)$$

$$q = \sin \theta_p \text{ and } \Delta q_i = \Delta(\sin \theta_p)_i \quad (5-16)$$

and (5-6) will be used to evaluate the partial derivatives. The definition of q in (5-16) is in part a notational convenience. But it also reflects the fact that it is the sine of the angle that is being estimated, not the angle; this choice of variable has significant consequences in the subsequent analysis.

From (5-10)

$$\Delta x_{i+1}^* = [(\partial x_D^* / \partial q) \Delta q_i] - [y_D^*(\partial y_D^* / \partial q) \Delta q_i + (z_T^* - z_D^*) \Delta z_{i+1}] / R_D \quad (5-17)$$

where

$$R_D = [\rho^2 - (y_D^*)^2 - (z_T^* - z_D^*)^2]^{1/2} = x_T^* - x_D^* \quad (5-18)$$

Next, from (5-11)

$$\Delta q_{i+1} = [(z_T^* / x_T^{*2}) \Delta z_{i+1} - (z_T^{*2} / x_T^{*3}) \Delta x_{i+1}] \sin \theta_C / R_q \quad (5-19)$$

where

$$R_q = [1 + z_T^{*2} / x_T^{*2}]^{1/2} \quad (5-20)$$

Finally, the partial derivatives of the geometrical constants with respect to the estimated sine of the azimuth angle are from (5-6). The zeros in the third row and column of (5-21) express formally the fact that

the geometrical parameters of altitude are independent of the rotation.

$$\begin{pmatrix} \partial x_D^*/\partial q & \partial x_E^*/\partial q \\ \partial y_D^*/\partial q & \partial y_E^*/\partial q \\ \partial z_D^*/\partial q & \partial z_E^*/\partial q \end{pmatrix} = \begin{pmatrix} -\tan\theta_p & -1 & 0 \\ 1 & -\tan\theta_p & 0 \\ 0 & 0 & 0 \end{pmatrix} \begin{pmatrix} x_D' & x_E' \\ y_D' & y_E' \\ z_D' & z_E' \end{pmatrix} \quad (5-21)$$

The matrices S and T may now be defined. The variables are taken in the following order:

1. Δz^* , from (5-14); this will appear in the third rows of S and T;
2. Δx^* , from (5-17); this will appear in the second rows of S and T;
3. Δq , from (5-19); this will appear in the first rows of S and T.

This sequence is consistent with the definition of the vector of variables as $[\Delta(\sin\theta_p) \quad \Delta x^* \quad \Delta z^*]^T$. Then the matrix S is

$$S = \begin{pmatrix} 1 & (z^{*2}/x^{*3})\sin\theta_C/R_q & (-z^*/x^{*2})\sin\theta_C/R_q \\ 0 & 1 & (z^*-z_D^*)/R_D \\ 0 & 0 & 1 \end{pmatrix} \quad (5-22)$$

There is a significant and deliberate similarity between (5-22) and (4-10). In both equations, the main diagonal elements are 1, and the zero and non-zero elements appear in the same locations. In harmony with the forecast, the consequence is that S^{-1} will have exactly the same form as in section 4.

The matrix T is

$$T = \begin{pmatrix} 0 & 0 & 0 \\ [(\partial x_D^*/\partial q) - (y_D^*/R_D)(\partial y_D^*/\partial q)] & 0 & 0 \\ [-(x^*-x_E^*)(\partial x_E^*/\partial q) = y_E^* \partial y_E^*/\partial q] \tan\phi/R_E & [(x^*-x_E^*) \tan\phi/R_E] & 0 \end{pmatrix} \quad (5-23)$$

There are further consequences of the definition of the variable as the estimate of $(\sin\theta_p)$:

- a. The zero and non-zero elements of T are in the same locations as in (4-11);
- b. The characteristic equation for the RGSi problem is identical in form to that of the RGSi problem expressed in (4-13);
- c. The expansion of the determinant of the RGSi characteristic equation has the same form as (4-14), and thus is

$$\Delta = \lambda\{\lambda^2 + \lambda[s_{23}t_{32} + s_{12}t_{21} - t_{31}(s_{12}s_{23} - s_{13})] + s_{13}t_{21}t_{32}\} = 0 \quad (5-24)$$

One eigenvalue of (5-24) is zero. The others are found from the quadratic term in (5-24), $\{\lambda^2 + B\lambda + C\}$, which is now examined under the simplifying assumption, used in section 4, of collocation of the ground units at the origin.

When the several units are collocated at the origin, the determinant simplifies much more than with the GSI in section 4. The geometry parameters vanish as $x_A = y_A = z_A = x_D = y_D = z_D = x_E = y_E = z_E = 0$, and thus $x_A' = y_A' = z_A' = x_D' = y_D' = z_D' = x_E' = y_E' = z_E' = 0$ in accordance with (5-5). And, since these translated parameters (x_A' , etc.) are all zero, then (5-6) shows that all of the rotated geometry elements, such as x_D^* , are all zero. Finally, (5-21) shows that the partial derivatives of the rotated geometry elements ($\partial x_A^* / \partial q$, etc.) also are all zero. With these values, (5-23) reduces to

$$\Delta = \lambda(\lambda^2 + \lambda \tan^2 \phi) = \lambda^2(\lambda + \tan^2 \phi) = 0 \quad (5-25)$$

and the three eigenvalues are $\lambda = 0$, $\lambda = 0$, and $\lambda = -\tan^2 \phi$ (5-26)

The meaning of this result is that the convergence rate, which is mostly determined by the eigenvalue of greatest magnitude, is completely independent of the observed azimuth angle, and is a function only of the elevation angle. The maximum elevation angle is 30° , and the corresponding eigenvalue is $-1/3$. If the resulting convergence rate is too slow, the process can be improved by using the sine-form of the elevation equation, (5-8). Alternately, it is possible to undertake a second translation of the origin, followed by a rotation about the y^* axis into the altitude direction; however, this seems not worth the effort to pursue further.

A very similar simple result is achieved under the more interesting assumption that the azimuth and DME units are collocated in a conventional split-site configuration, with the elevation antenna at the conventional location. In this case the term $s_{13}t_{21}t_{32}$ in (5-24) is zero since the partial derivatives in t_{21} are zero. Therefore, two eigenvalues are zero. If it be assumed that the three ground units are at the same altitude so that $z_A = z_D = z_E$, then the third eigenvalue is

$$\lambda = -\{ [(x^* - x_E^*)/x^*] + [(x^* - x_E^*)(\partial x_E^* / \partial q) - y_E^*(\partial y_E^* / \partial q)](\sin \theta_p / x^{*2}) \} \tan^2 \phi \quad (5-27)$$

and this eigenvalue converges towards $(-\tan^2 \phi)$ as x^* becomes large compared to x_E^* . And, in any case, the value cannot be far from $(-\tan^2 \phi)$.

The analysis of the sine form of the altitude equation, (5-4), is presented in appendix C.

SECTION 6

COMPARISONS OF PERFORMANCE

Table 6-1 compares various statistical elements of the characteristics and performance of this RGSi PRA against the GSI presented in section 4 and also against an equivalent Newton-Raphson approach.

A Newton-Raphson PRA was presented in [4] as an alternate to the algorithm offered in [2] as Case 12, because it combines compactness, performance, and a relatively small computational burden. It is used here for comparisons, and, here and in [4], is designated as Newton-Raphson Alternate (NRA). See appendix B for an outline of its principles.

However, these algorithms used different initializations in the various sources referenced; a common form of initialization is used in this report to enable proper comparisons. The initialization used herein is: $x_0 = \rho \cos \theta$, $y_0 = -\rho \sin \theta$ and $z_0 = \rho \sin \phi$, where the initial values of x_0 and y_0 are required for the prototype GSI, while the NRA and the proposed RGSi also require z_0 ; see also [2]. The comparisons are in terms of:

- a. Lines of FORTRAN 77 code, as a measure of the required storage;
- b. The mean and standard deviation of the number of iterations to converge to the accuracy criterion ($x_T/10,000$) cited above in section 3, as a measure of speed;
- c. The number of products and quotients, and the number of transcendental operations (trigonometrical and square-root), inside the iterative loop as measures of the complexity.

Table 6-1. Comparison of Various PRAs

Property	RGSi	GSI	NRA
Lines	44	35	48
Mean Iterations	2.72	4.18*	2.00
Std. Dev., Iterations	0.88	1.48*	0.56
* or ÷ in Loop	22	9	65
Transcends. in Loop	4	1	2

* Note that the GSI diverges or is slow in 140 of the 250 cases in the database.

The RGSi requires more storage than the GSi and slightly less than the NRA; it can be further compacted if required. It converges faster than the GSi, wherever the GSi converges; it is important to recall that a principal motivation for this study was that the GSi PRA diverges within the MLS coverage, as was demonstrated in table 4-1. The RGSi converges approximately one iteration slower than the NRA.

The RGSi has about twice as many products or quotients in the iterative loop as the GSi, but has only $1/3$ of these operations compared to the NRA. The number of transcendental operations in the iterative loops differ for the three PRAs. If it be assumed that a transcendental operation is equivalent to five products, then the GSi has 14 products, the RGSi has approximately 42 products, and the NRA has 75 products. The product of the mean number of iterations to convergence with the number of products may be taken as a crude measure of the computational burden. From this viewpoint, the iterative computational burden of the RGSi is about thrice that of the GSi, but only about half that of the NRA. Other Newton-Raphson formulations exist, as in [2] and [4]; the NRA used herein is the smallest of these in terms of size, and the number of operations, false solutions and singularities.

The data presented in this table show that the RGSi is clearly superior to the equivalent GSi without rotation, as the GSi diverges, or converges slowly, in many areas within the MLS coverage. Further, the RGSi has a smaller computational burden than the NRA, while its convergence speed is almost equal to that of the NRA. It thus appears to be superior to the NRA.

LIST OF REFERENCES

1. International Civil Aeronautics Association, April 1985, (Correction as of October 22, 1987), "International Standards, Recommended Practices and Procedures for Air Navigation Services; Aeronautical Communications, Annex 10," Fourth Edition of Volume I, Montreal, Canada.
2. Radio Technical Commission for Aeronautics, 18 March 1988, "Minimum Operational Performance Standards for Airborne MLS Area Navigation Equipment," RTCA/DO-198, Appendix D, Washington, D.C.
3. Strang, G., 1980, Linear Algebra and Its Applications, Second Edition, New York, NY: Academic Press, page 380.
4. Hall, J. W., P. M. Hatzis, and F. D. Powell, June 1990, "Examination of the RTCA/DO-198 Position Reconstruction Algorithms for Area Navigation with the Microwave Landing System," ESD-TR-90-308, Electronic Systems Division, AFSC, Hanscom Air Force Base, MA.
5. United States Department of Transportation, Federal Aviation Agency, Program Engineering and Maintenance Service, October 1987, "Introduction to MLS," Washington, D.C.

APPENDIX A

FORTRAN 77 COMPUTER CODE

Line #	State	Code
1		SUBROUTINE AGR1(XD,YD,ZD,XA,YA,ZA,XE,YE,ZE,RHO,THETA,PHI
2		1 ,XT,YT,ZT,I56,ITER,ARAOUT,IFLAG)
3		DIMENSION ARAOUT(3,10)
4	C	STORE TRUE POSITION IN OUTPUT ARRAY; DON'T INCLUDE IN LINE-COUNT.
5		ARAOUT(1,1)=XT
6		ARAOUT(2,1)=YT
7		ARAOUT(3,1)=ZT
8	C	
9	C	ALGORITHM BEGINS HERE; FOR NOTATION SEE SECTION 3 IN TEXT.
10	C	TRIG FUNCTION ABBREVIATIONS; POSTSCRIPT "M" IMPLIES MEASURED ANGLE.
11		STM=SIN(THETA)
12		CTM=COS(THETA)
13		SPHIM=SIN(PHI)
14	C	INITIALIZATION; SEE ALSO [2] AND [3]. "HAT"=POSITION-ESTIMATE.
15		XHAT=XD+RHO*CTM
16		YHAT=YA-RHO*STM
17		ZHAT=ZE+RHO*SPHIM
18	C	INITIALIZE SINE & COSINE OF ROTATION-ANGLE ESTIMATE.
19	C	POSTSCRIPT "H" IMPLIES ROTATION-ANGLE SIN & COS ESTIMATES.
21		STH=STM
22		CTH=CTM
23	C	STORE INITIALIZATION OF POSITION ESTIMATE IN OUTPUT ARRAY;
24	C	DON'T COUNT THAT STORAGE AS PART OF LINE-COUNT.
25		ARAOUT(1,2)=XHAT
26		ARAOUT(2,2)=YHAT
27		ARAOUT(3,2)=ZHAT
29	C	TRANSLATIONS TO AZIMUTH ANTENNA SITE; SEE (5-5) IN TEXT.
29	C	SUBSCRIPT P=PRIME SIGNIFIES TRANSLATION, & R SIGNIFIES ROTATION.
30	C	NOTE THAT ZDPR=ZDP & ZEPR=ZEP, & THUS DON'T NEED SEPARATE LINES.
31		XDP=XD-XA
32		YDP=YD-YA
33		ZDPR=ZD-ZA
34		XEP=XE-XA
35		YEP=YE-YA
36		ZEPR=ZE-ZA
37		XHATP=XHAT-XA
38		YHATP=YHAT-YA
39		ZHATPR=ZHAT-ZA

Figure A-1. Computer Code


```

40 C      Z-COMPONENTS DON'T NEED ROTATION; SEE (5-6).
41 C      INITIAL X & Z ARE NEEDED IN TRANSLATED-ROTATED COORDINATES.
42      XHATPR=XHATP*CTH-YHATP*STH
43 C      FOR INITIAL Z USE ZHATPR FROM LINE 39, ABOVE.
44 C      START OF ITERATION LOOP
45      DO 420 I=1,ITER
46 C      ROTATIONS; SEE (5-6).  ZDPR & ZEPR ARE COMPUTED OUTSIDE THE LOOP.
47      XDPR=XDP*CTH-YDP*STH
48      YDPR=XDP*STH+YDP*CTH
49      XEPR=XEP*CTH-YEP*STH
50      YEPR=XEP*STH+YEP*CTH
51 C      COMPUTE Z & X IN ROTATED COORDS; SEE (5-8) & (5-10).
52      ZHATPR=ZEPR+SQRT((XHATPR-XEPR)**2+YEPR**2+(ZHATPR-ZEPR)**2)*SPHIM
53      RAD=RHO**2-YDPR**2-(ZHATPR-ZDPR)**2
54 C      NEGATIVE RADICAND TRAP AND SIGNAL THEREOF FOLLOW.
55      IF(RAD .GE. 0.0)GOTO 421
56      GOTO 422
57 421    XHATPR=XDPR+SQRT(RAD)
58      IFLAG=1
59 C      RECOMPUTE THE AZ ANGLE'S SINE & COSINE, SEE (5-11).
60 C      I56=0 FOR CONICAL, =1 FOR PLANAR; SEE [1], P.150B, NOTE 2.
61      STH=STM*SQRT(1.0+(1-I56)*(ZHATPR/XHATPR)**2)
62      CTH=SQRT(1.0-STH**2)
63 C      DEROTATIONS (5-12) AND DE-TRANSLATION; THESE GO OUTSIDE THE LOOP &
63 C      ARE HERE FOR PRINTOUT.  DON'T COUNT THE STORAGE LINES.
64      XHATP=XHATPR*CTH
65      YHATP=-XHATPR*STH
66 C      DE-TRANSLATIONS; SEE (5-13).
67      XHAT=XHATP+XA
68      YHAT=YHATP+YA
69      ZHAT=ZHATPR+ZA
70      GOTO 423
71 422    XHAT=0.0
72      YHAT=0.0
73      ZHAT=0.0
74      IFLAG=2
75 423    ARAOUT(1,(2+I))=XHAT
56      ARAOUT(2,(2+I))=YHAT
77      ARAOUT(3,(2+I))=ZHAT
78 C      THIS COMPLETES THE ITERATION.  420 IS END OF ITERATION LOOP.
79 420    CONTINUE
80      RETURN
81      END

```

Figure A-1. Computer Code (concluded)

APPENDIX B

ALTERNATE NEWTON-RAPHSON ALGORITHM

An Newton-Raphson approach to forming an MLS PRA was used to form a basis for comparison with the RGSI which is the subject of this report. The derivation of the alternate form, NRA, is presented here, to make this report more self-contained.

The Newton-Raphson approach for a three-dimensional problem first forms a vector, \underline{F} , from the system equations; its three components are to be simultaneously zero at the solution. This procedure then increments the vector of estimates, \underline{X} , according to the matrix product

$$\Delta \underline{X}_{i+1} = J^{-1} \underline{F}_i \quad (B-1)$$

where J is the (Jacobian) matrix of the partial derivatives of the vector \underline{F} with respect to the vector of variable, \underline{X} , and the right-hand side is evaluated at iteration i . The process fails if the matrix J is singular, (when its determinant equals zero), and it may yield false solutions or fail in other ways, such as extreme sensitivity to round-off errors, if the estimate is at any point in the iteration near a singularity. The NR approach also may fail to converge, or converge to a wrong solution if the desired solution is separated by a maximum or a minimum, or a point of inflection, from the (x_T, y_T, z_T) triple of the solution at any point in the iteration. Initial conditions are required for x , y , and z ; their selection determines which of the multiple solutions will be found. This concept is now applied to the MLS problem.

In this NRA approach, the vector of variables, \underline{X} , is the set of variables x , y and z , and the vector \underline{F} is defined by f , g and h where

$$f = (1/2)[(x-x_D)^2 + (y-y_D)^2 + (z-z_D)^2 - \rho^2] \quad (B-2)$$

$$g = (y-y_A)\cos\theta + [(x-x_A)^2 + (z-z_A)^2]^{1/2}\sin\theta \quad (B-3)$$

$$h = (z-z_E)\cos\phi - [(x-x_E)^2 + (y-y_E)^2]^{1/2}\sin\phi \quad (B-4)$$

The Jacobian matrix of partial derivatives is

$$J = \begin{pmatrix} (x-x_D) & (y-y_D) & (z-z_D) \\ (x-x_A)\sin\theta/R_A & \cos\theta & (z-z_A)\sin\theta/R_A \\ -(x-x_E)\sin\phi/R_E & -(y-y_E)\sin\phi/R_E & \cos\phi \end{pmatrix} \quad (B-5)$$

where $R_A = [(x-x_A)^2 + (z-z_A)^2]^{1/2}$, and $R_E = [(x-x_E)^2 + (y-y_E)^2]^{1/2}$.

This algorithm is believed to have the minimum possible number of false solutions. It has one condition in which the matrix J is singular,

which precludes solution. This is now considered.

Assume the ground units are arranged so that $x_A = x_D = x_E$. Then the factor $(x - x_E)$ appears everywhere in the first column of (B-5), and the matrix is singular when the aircraft is at a location such that $x = x_E$. This surface tends to be nearly-vertical, with its concave face towards the stop-end of the runway. The surface is thus out of coverage.

APPENDIX C

THE SINE FORM OF THE RGSI

This form yields a slight, but worthwhile, improvement of the speed of convergence of the RGSI. Instead of (5-1), use (5-4), rewritten as

$$z_{i+1}^* = z_E + [(x_i^* - x_E^*)^2 + (y_i^* - y_E^*)^2 + (z_i^* - z_E^*)^2]^{1/2} \sin \phi \quad (C-1)$$

With this change, the matrix S is unchanged, while the third column of matrix T becomes $(0 \ 0 \ t_{33})^T$ where

$$t_{33} = [(z_T^* - z_E^*) \sin \phi / R_E] \quad (C-2)$$

and R_E is redefined as

$$R_E = [(x_T^* - x_E^*)^2 + (y_E^*)^2 + (z_T^* - z_E^*)^2]^{1/2} \quad (C-3)$$

The third column of the determinant $|I\lambda - S^{-1}T|$ becomes

$$\{ [-(s_{12}s_{23} - s_{13})t_{33}] \ [s_{23}t_{33}] \ [\lambda - t_{33}] \}^T \quad (C-4)$$

and the characteristic equation, replacing (5-24), is

$$\Delta = \lambda \{ \lambda^2 + [s_{23}t_{32} + s_{12}t_{21} - (s_{12}s_{23} - s_{13})t_{31} - t_{33}] \lambda + [s_{13}t_{21}t_{32} - s_{12}t_{21}t_{33}] \} = 0 \quad (C-5)$$

One eigenvalue is zero, while the other two are found from the quadratic factor in (C-5).

The simplifying assumption that the three ground units are collocated at the origin reduces (C-5) to

$$\Delta = \lambda^2 \{ \lambda + s_{23}t_{32} - t_{33} \} = 0 \quad (C-6)$$

since $t_{21} = t_{31} = 0$, as shown in section 5. Then the non-zero eigenvalue is

$$\lambda = t_{33} - s_{23}t_{32} = [(z_T^* - z_E^*) \sin \phi / R_E] - [(z_T^* - z_D^*) / R_D] [(x_T^* - x_E^*) \sin \phi / R_E]$$

which reduces to

$$\lambda = [\sin^2 \phi] - [\tan \phi][\sin \phi \cos \phi] = \sin^2 \phi - \sin^2 \phi = 0. \quad (C-7)$$

It thus develops that all three eigenvalues are zero in the collocated case. This happy result is confirmed by the data presented on the first two pages of the exercise in appendix D.

APPENDIX D

EXERCISE OF THE RGSI

The conical-azimuth form of this algorithm, defined in appendix C, was tested and exercised in a simulation. Five different arrangements of the ground units were selected. The first assumes that all units are collocated at the usual site for the elevation antenna, the second assumes a conventional split-site with the DME collocated with the azimuth antenna at the usual location of the latter, and the third assumes a split-site but with the DME collocated with the elevation antenna as suggested in [8]. The fourth and fifth arrangements assume that all three units are separated, in order to test the ability of the algorithm to handle general sites correctly.

The aircraft was assumed to be at 75 different locations which span the possibilities of range, azimuth and elevation conditions within the MLS coverage. The algorithm was tested at each aircraft location for all five of the ground unit arrangements, so that there is a total of 375 tests.

A small sample of these tests is presented in this appendix, consisting of ten aircraft locations at each of the five ground unit arrangements. The structure of the tables is the same as in tables 1 through 4. The heading for each page gives the positions of the ground units, and the five sets below present the components of aircraft location estimate for five different aircraft locations. The first column in each set is the true location of the aircraft, the second column is the initial condition estimate, and the following six columns show the behavior of the algorithm at six successive iterations. The error may be determined in any case by comparing the estimated location after an iteration with the true location in column 1.

Several comments on the characteristics of the algorithm are offered. In the entire database of 375 tests there is no case in which the negative-radical condition was encountered, although this was common with the GSI; see the code in appendix A, above Statement 421. There is no case in which the algorithm diverged, nor any in which it required more than five iterations to meet the accuracy criterion of $|\epsilon|_{\max} < (x_T/10,000)$.

The initial conditions for the database are

$$x_0 = x_D + \rho \cos \theta \quad (D-1)$$

$$y_0 = y_A - \rho \sin \theta \quad (D-2)$$

$$z_0 = z_E + \rho \sin \phi \quad (D-3)$$

Performance of the RGSI without x_D , y_A and z_E may be seen in [7].

Table D-1. Rotational Algorithm Exercise

GROUND STATION SITE GEOMETRY # 1								
AZIMUTH ANTENNA SITE			DME TRANSMITTER SITE			ELEVATION ANTENNA SITE		
X	Y	Z	X	Y	Z	X	Y	Z
-1000.	500.	5.	-1000.	500.	5.	-1000.	500.	5.
AIRCRAFT POSITION #1. OBSERVED DATA: RHO=11628.4 THETA=-54.78 PHI=14.93								
TRUE POS. INIT. EST.								
ITERATION NUMBER I	1	2	3	4	5	6		
X	5000.00	5705.97	4950.21	5000.00	5000.00	5000.00	5000.00	5000.00
Y	10000.00	10000.00	10000.00	10000.00	10000.00	10000.00	10000.00	10000.00
Z	3000.00	3000.00	3097.74	3000.00	3000.00	3000.00	3000.00	3000.00
AIRCRAFT POSITION #6. OBSERVED DATA: RHO=6102.5 THETA= -4.70 PHI=9.38								
TRUE POS. INIT. EST.								
ITERATION NUMBER I	1	2	3	4	5	6		
X	5000.00	5081.94	4997.81	5000.00	5000.00	5000.00	5000.00	5000.00
Y	1000.00	1000.00	1000.00	1000.00	1000.00	1000.00	1000.00	1000.00
Z	1000.00	1000.00	1013.14	1000.00	1000.00	1000.00	1000.00	1000.00
AIRCRAFT POSITION #11. OBSERVED DATA: RHO=22742.3 THETA=-59.03 PHI=10.12								
TRUE POS. INIT. EST.								
ITERATION NUMBER I	1	2	3	4	5	6		
X	10000.00	10702.99	9977.59	10000.00	10000.00	10000.00	10000.00	10000.00
Y	20000.00	20000.00	20000.00	20000.00	20000.00	20000.00	20000.00	20000.00
Z	4000.00	4000.00	4061.17	4000.00	4000.00	4000.00	4000.00	4000.00
AIRCRAFT POSITION #16. OBSERVED DATA: RHO=11926.4 THETA=-22.17 PHI=-.79								
TRUE POS. INIT. EST.								
ITERATION NUMBER I	1	2	3	4	5	6		
X	10000.00	10044.91	9999.69	10000.00	10000.00	10000.00	10000.00	10000.00
Y	5000.00	5000.00	5000.00	5000.00	5000.00	5000.00	5000.00	5000.00
Z	1000.00	1000.00	1003.46	1000.00	1000.00	1000.00	1000.00	1000.00
AIRCRAFT POSITION #21. OBSERVED DATA: RHO=47552.1 THETA=-56.17 PHI=6.03								
TRUE POS. INIT. EST.								
ITERATION NUMBER I	1	2	3	4	5	6		
X	25000.00	25475.46	24994.71	25000.00	25000.00	25000.00	25000.00	25000.00
Y	40000.00	40000.00	40000.00	40000.00	40000.00	40000.00	40000.00	40000.00
Z	5000.00	5000.00	5027.48	5000.00	5000.00	5000.00	5000.00	5000.00

Table D-1. Rotational Algorithm Exercise (continued)

GROUND STATION SITE GEOMETRY # 1								
AZIMUTH ANTENNA SITE			DME TRANSMITTER SITE			ELEVATION ANTENNA SITE		
X	Y	Z	X	Y	Z	X	Y	Z
-1000.	500.	5.	-1000.	500.	5.	-1000.	500.	5.

AIRCRAFT POSITION #26. OBSERVED DATA: RHO=27793.4 THETA=-19.99 PHI=5.15								
TRUE POS. INIT. EST.								
ITERATION NUMBER I	1	2	3	4	5	6		
X	25000.00	25119.44	24999.04	25000.00	25000.00	25000.00	25000.00	25000.00
Y	10000.00	10000.00	10000.00	10000.00	10000.00	10000.00	10000.00	10000.00
Z	2500.00	2500.00	2510.03	2500.00	2500.00	2500.00	2500.00	2500.00

AIRCRAFT POSITION #31. OBSERVED DATA: RHO=90835.8 THETA=-55.10 PHI=6.32								
TRUE POS. INIT. EST.								
ITERATION NUMBER I	1	2	3	4	5	6		
X	50000.00	50970.18	49988.14	50000.00	50000.00	50000.00	50000.00	50000.00
Y	75000.00	75000.01	75000.00	75000.00	75000.00	75000.00	75000.00	75000.00
Z	10000.00	10000.00	10060.33	10000.00	10000.00	10000.00	10000.00	10000.00

AIRCRAFT POSITION #36. OBSERVED DATA: RHO=90835.8 THETA=-55.10 PHI=6.32								
TRUE POS. INIT. EST.								
ITERATION NUMBER I	1	2	3	4	5	6		
X	50000.00	50970.18	49988.14	50000.00	50000.00	50000.00	50000.00	50000.00
Y	75000.00	75000.01	75000.00	75000.00	75000.00	75000.00	75000.00	75000.00
Z	10000.00	10000.00	10060.33	10000.00	10000.00	10000.00	10000.00	10000.00

AIRCRAFT POSITION #41. OBSERVED DATA: RHO=129193.8 THETA=-43.85 PHI=8.90								
TRUE POS. INIT. EST.								
ITERATION NUMBER I	1	2	3	4	5	6		
X	90000.00	92170.81	89947.37	90000.00	90000.00	90000.00	90000.00	90000.00
Y	90000.00	89999.99	89999.99	90000.00	90000.00	90000.00	90000.00	90000.00
Z	20000.00	20000.00	20238.05	20000.00	20000.00	20000.00	20000.00	20000.00

AIRCRAFT POSITION #46. OBSERVED DATA: RHO=103611.0 THETA=-28.54 PHI=1.10								
TRUE POS. INIT. EST.								
ITERATION NUMBER I	1	2	3	4	5	6		
X	90000.00	90021.86	89999.99	90000.00	90000.00	90000.00	90000.00	90000.00
Y	50000.00	50000.00	50000.00	50000.00	50000.00	50000.00	50000.00	50000.00
Z	2000.00	2000.00	2000.37	2000.00	2000.00	2000.00	2000.00	2000.00

Table D-1. Rotational Algorithm Exercise (continued)

GROUND STATION SITE GEOMETRY # 2								
AZIMUTH ANTENNA SITE			DME TRANSMITTER SITE			ELEVATION ANTENNA SITE		
X	Y	Z	X	Y	Z	X	Y	Z
-6000.	0.	5.	-6000.	0.	5.	-1000.	500.	5.

AIRCRAFT POSITION #1. OBSERVED DATA: RHO=15164.8 THETA=-41.26 PHI=14.93								
TRUE POS. INIT. EST.								
ITERATION NUMBER I	1	2	3	4	5	6		
X	5000.00	5400.44	4966.02	4998.98	4999.97	5000.00	5000.00	5000.00
Y	10000.00	10000.00	10000.00	10000.00	10000.00	10000.00	10000.00	10000.00
Z	3000.00	3910.82	3122.11	3003.76	3000.11	3000.00	3000.00	3000.00

AIRCRAFT POSITION #6. OBSERVED DATA: RHO=11090.1 THETA=-5.17 PHI=9.38								
TRUE POS. INIT. EST.								
ITERATION NUMBER I	1	2	3	4	5	6		
X	5000.00	5044.91	4996.59	4999.96	5000.00	5000.00	5000.00	5000.00
Y	1000.00	1000.00	1000.00	1000.00	1000.00	1000.00	1000.00	1000.00
Z	1000.00	1813.23	1036.99	1000.46	1000.01	1000.00	1000.00	1000.00

AIRCRAFT POSITION #11. OBSERVED DATA: RHO=25922.2 THETA=-50.49 PHI=10.12								
TRUE POS. INIT. EST.								
ITERATION NUMBER I	1	2	3	4	5	6		
X	10000.00	10491.21	9984.73	9999.85	10000.00	10000.00	10000.00	10000.00
Y	20000.00	20000.00	20000.00	20000.00	20000.00	20000.00	20000.00	20000.00
Z	4000.00	4558.60	4060.65	4000.59	4000.01	4000.00	4000.00	4000.00

AIRCRAFT POSITION #16. OBSERVED DATA: RHO=16792.6 THETA=-17.32 PHI=4.79								
TRUE POS. INIT. EST.								
ITERATION NUMBER I	1	2	3	4	5	6		
X	10000.00	10030.91	9999.64	10000.00	10000.00	10000.00	10000.00	10000.00
Y	5000.00	5000.00	5000.00	5000.00	5000.00	5000.00	5000.00	5000.00
Z	1000.00	1405.97	1005.77	1000.01	1000.00	1000.00	1000.00	1000.00

AIRCRAFT POSITION #21. OBSERVED DATA: RHO=50852.2 THETA=-51.87 PHI= 6.03								
TRUE POS. INIT. EST.								
ITERATION NUMBER I	1	2	3	4	5	6		
X	25000.00	25399.84	24995.63	24999.99	25000.00	25000.00	25000.00	25000.00
Y	40000.00	40000.00	40000.00	40000.00	40000.00	40000.00	40000.00	40000.00
Z	5000.00	5346.66	5027.03	5000.05	5000.00	5000.00	5000.00	5000.00

Table D-1. Rotational Algorithm Exercise (continued)

GROUND STATION SITE GEOMETRY # 2								
AZIMUTH ANTENNA SITE			DME TRANSMITTER SITE			ELEVATION ANTENNA SITE		
X	Y	Z	X	Y	Z	X	Y	Z
-6000.	0.	5.	-6000.	0.	5.	-1000.	500.	5.
AIRCRAFT POSITION #26. OBSERVED DATA: RHO=32668.4 THETA=-17.82 PHI=5.15								
TRUE POS. INIT. EST.								
ITERATION NUMBER I	1	2	3	4	5	6		
X	25000.00	25100.24	24999.01	25000.00	25000.00	25000.00	25000.00	25000.00
Y	10000.00	10000.00	10000.00	10000.00	10000.00	10000.00	10000.00	10000.00
Z	2500.00	2937.62	2512.24	2500.02	2500.00	2500.00	2500.00	2500.00
AIRCRAFT POSITION #31. OBSERVED DATA: RHO=94132.4 THETA=-52.82 PHI=6.32								
TRUE POS. INIT. EST.								
ITERATION NUMBER I	1	2	3	4	5	6		
X	50000.00	50884.97	49989.36	49999.99	50000.00	50000.00	50000.00	50000.00
Y	75000.00	75000.00	75000.00	74999.99	74999.99	74999.99	74999.99	74999.99
Z	10000.00	10362.73	10059.44	10000.06	10000.00	10000.00	10000.00	10000.00
AIRCRAFT POSITION #36. OBSERVED DATA: RHO=94132.4 THETA=-52.82 PHI=6.32								
TRUE POS. INIT. EST.								
ITERATION NUMBER I	1	2	3	4	5	6		
X	50000.00	50884.97	49989.36	49999.99	50000.00	50000.00	50000.00	50000.00
Y	75000.00	75000.00	75000.00	74999.99	74999.99	74999.99	74999.99	74999.99
Z	10000.00	10362.73	10059.44	10000.06	10000.00	10000.00	10000.00	10000.00
AIRCRAFT POSITION #41. OBSERVED DATA: RHO=133100.7 THETA=-42.55 PHI=8.90								
TRUE POS. INIT. EST.								
ITERATION NUMBER I	1	2	3	4	5	6		
X	90000.00	92060.20	89949.63	89999.95	90000.02	90000.02	90000.02	90000.02
Y	90000.00	90000.00	90000.00	90000.00	90000.00	90000.00	90000.00	90000.00
Z	20000.00	20604.66	20240.39	20000.30	20000.00	20000.00	20000.00	20000.00
AIRCRAFT POSITION #46. OBSERVED DATA: RHO=108258.9 THETA=-27.51 PHI=1.10								
TRUE POS. INIT. EST.								
ITERATION NUMBER I	1	2	3	4	5	6		
X	90000.00	90020.73	89999.99	90000.00	90000.00	90000.00	90000.00	90000.00
Y	50000.00	50000.00	50000.00	50000.00	50000.00	50000.00	50000.00	50000.00
Z	2000.00	2089.49	2000.38	2000.00	2000.00	2000.00	2000.00	2000.00

Table D-1. Rotational Algorithm Exercise (continued)

GROUND STATION SITE GEOMETRY # 3

AZIMUTH ANTENNA SITE			DME TRANSMITTER SITE			ELEVATION ANTENNA SITE		
X	Y	Z	X	Y	Z	X	Y	Z
-6000.	-1000.	10.	-1000.	500.	5.	-1000.	500.	5.

AIRCRAFT POSITION #1. OBSERVED DATA: RHO=11628.4 THETA=-43.98 PHI=14.93
TRUE POS. INIT. EST.

ITERATION NUMBER I	1	2	3	4	5	6
X	5000.00	7367.72	5075.96	4998.73	4999.17	5000.00
Y	10000.00	7074.73	10047.20	10002.34	9999.54	9999.97
Z	3000.00	3000.00	2904.97	3013.88	3001.25	2999.87

AIRCRAFT POSITION #6. OBSERVED DATA: RHO=6102.5 THETA=-10.26 PHI=9.38
TRUE POS. INIT. EST.

ITERATION NUMBER I	1	2	3	4	5	6
X	5000.00	5004.80	5003.37	4999.98	5000.00	5000.00
Y	1000.00	87.39	1000.20	999.99	1000.00	1000.00
Z	1000.00	1000.00	974.86	999.88	999.99	1000.00

AIRCRAFT POSITION #11. OBSERVED DATA: RHO=22742.3 THETA=-51.86 PHI=10.12
TRUE POS. INIT. EST.

ITERATION NUMBER I	1	2	3	4	5	6
X	10000.00	13045.39	10061.37	9999.67	9999.71	10000.00
Y	20000.00	16886.79	20043.47	20002.22	19999.81	19999.99
Z	4000.00	4000.00	3893.25	4008.52	4000.57	3999.97

AIRCRAFT POSITION #16. OBSERVED DATA: RHO=11926.4 THETA=-20.52 PHI=4.79
TRUE POS. INIT. EST.

ITERATION NUMBER I	1	2	3	4	5	6
X	10000.00	10169.70	10003.65	10000.02	10000.00	10000.00
Y	5000.00	3180.64	5000.46	5000.01	5000.00	5000.00
Z	1000.00	1000.00	960.19	1000.02	1000.00	1000.00

AIRCRAFT POSITION #21. OBSERVED DATA: RHO=47552.1 THETA=-52.55 PHI=6.03
TRUE POS. INIT. EST.

ITERATION NUMBER I	1	2	3	4	5	6
X	25000.00	27912.30	25026.88	25000.10	24999.98	25000.00
Y	40000.00	36752.87	40016.89	40000.57	39999.99	40000.00
Z	5000.00	5000.00	4913.61	5002.07	5000.08	5000.00

Table D-1. Rotational Algorithm Exercise (continued)

GROUND STATION SITE GEOMETRY # 3								
AZIMUTH ANTENNA SITE			DME TRANSMITTER SITE			ELEVATION ANTENNA SITE		
X	Y	Z	X	Y	Z	X	Y	Z
-6000.	-1000.	10.	-1000.	500.	5.	-1000.	500.	5.
AIRCRAFT POSITION #26. OBSERVED DATA: RHO=27793.4 THETA=-19.48 PHI=5.15								
TRUE POS. INIT. EST.								
ITERATION NUMBER I	1	2	3	4	5	6		
X	25000.00	25202.70	25003.52	25000.01	25000.00	25000.00	25000.00	25000.00
Y	10000.00	8267.88	10000.27	10000.00	10000.00	10000.00	10000.00	10000.00
Z	2500.00	2500.00	2465.42	2500.03	2500.00	2500.00	2500.00	2500.00
AIRCRAFT POSITION #31. OBSERVED DATA: RHO=90835.8 THETA=-53.19 PHI=6.32								
TRUE POS. INIT. EST.								
ITERATION NUMBER I	1	2	3	4	5	6		
X	50000.00	53430.50	50026.59	49999.73	49999.99	50000.00	50000.00	50000.00
Y	75000.00	71721.88	75019.75	75000.26	74999.99	75000.00	75000.00	75000.00
Z	10000.00	10000.00	9934.87	10002.64	10000.04	10000.00	10000.00	10000.00
AIRCRAFT POSITION #36. OBSERVED DATA: RHO=90835.8 THETA=-53.19 PHI=6.32								
TRUE POS. INIT. EST.								
ITERATION NUMBER I	1	2	3	4	5	6		
X	50000.00	53430.50	50026.59	49999.73	49999.99	50000.00	50000.00	50000.00
Y	75000.00	71721.88	75019.75	75000.26	74999.99	75000.00	75000.00	75000.00
Z	10000.00	10000.00	9934.87	10002.64	10000.04	10000.00	10000.00	10000.00
AIRCRAFT POSITION #41. OBSERVED DATA: RHO=129193.8 THETA=-42.86 PHI=8.90								
TRUE POS. INIT. EST.								
ITERATION NUMBER I	1	2	3	4	5	6		
X	90000.00	93698.86	90000.78	89998.99	90000.00	90000.00	90000.00	90000.00
Y	90000.00	86881.60	90016.86	89999.84	89999.99	89999.99	89999.99	89999.99
Z	20000.00	20000.00	20085.17	20003.94	19999.97	20000.00	20000.00	20000.00
AIRCRAFT POSITION #46. OBSERVED DATA: RHO=103611.0 THETA=-27.97 PHI=1.10								
TRUE POS. INIT. EST.								
ITERATION NUMBER I	1	2	3	4	5	6		
X	90000.00	90504.79	90000.36	90000.00	90000.00	90000.00	90000.00	90000.00
Y	50000.00	47601.48	50000.05	50000.00	50000.00	50000.00	50000.00	50000.00
Z	2000.00	2000.00	1986.92	2000.00	2000.00	2000.00	2000.00	2000.00

Table D-1. Rotational Algorithm Exercise (continued)

GROUND STATION SITE GEOMETRY # 3

AZIMUTH ANTENNA SITE			DME TRANSMITTER SITE			ELEVATION ANTENNA SITE		
X	Y	Z	X	Y	Z	X	Y	Z
-1000.	-500.	5.	-5000.	-1000.	25.	-1000.	500.	5.

AIRCRAFT POSITION #1. OBSERVED DATA: RHO=15160.8 THETA=-57.44 PHI=14.93
TRUE POS. INIT. EST.

ITERATION NUMBER I	1	2	3	4	5	6		
X	5000.00	3160.38	4772.59	5033.49	4994.05	5000.87	4999.85	5000.02
Y	10000.00	12277.28	9906.24	10027.09	9997.46	10000.68	9999.93	1000.00
Z	3000.00	3509.80	3298.58	2971.38	3008.27	2999.22	3000.21	2999.98

AIRCRAFT POSITION #6. OBSERVED DATA: RHO=10244.5 THETA=-13.85 PHI=9.38
TRUE POS. INIT. EST.

ITERATION NUMBER I	1	2	3	4	5	6	
X	5000.00	4946.50	4993.67	5000.06	5000.00	5000.00	5000.00
Y	1000.00	1953.12	1000.60	1000.03	1000.00	1000.00	1000.00
Z	1000.00	1675.36	1051.63	1000.40	1000.02	1000.00	1000.00

AIRCRAFT POSITION #11. OBSERVED DATA: RHO=26111.3 THETA=-60.28 PHI=10.12
TRUE POS. INIT. EST.

ITERATION NUMBER I	1	2	3	4	5	6		
X	10000.00	7945.42	9897.56	10008.60	9999.23	10000.07	9999.99	10000.00
Y	20000.00	22176.35	19936.16	20006.46	19999.52	20000.05	20000.00	20000.00
Z	4000.00	4591.82	4170.50	3987.09	4001.31	3999.90	4000.01	4000.00

AIRCRAFT POSITION #16. OBSERVED DATA: RHO=16184.9 THETA=-26.47 PHI=4.79
TRUE POS. INIT. EST.

ITERATION NUMBER I	1	2	3	4	5	6	
X	10000.00	9487.97	9996.43	10000.09	10000.00	10000.00	10000.00
Y	5000.00	6714.53	4999.52	5000.04	5000.00	5000.00	5000.00
Z	1000.00	1355.27	1028.33	999.91	1000.01	1000.00	1000.00

AIRCRAFT POSITION #21. OBSERVED DATA: RHO=51046.6 THETA=-56.83 PHI=6.03
TRUE POS. INIT. EST.

ITERATION NUMBER I	1	2	3	4	5	6		
X	25000.00	22931.27	24971.16	25000.93	24999.97	25000.00	25000.00	25000.00
Y	40000.00	42226.98	39980.24	40000.68	39999.98	40000.00	40000.00	40000.00
Z	5000.00	5367.07	5080.91	4997.52	5000.08	5000.00	5000.00	5000.00

Table D-1. Rotational Algorithm Exercise (continued)

GROUND STATION SITE GEOMETRY # 4								
AZIMUTH ANTENNA SITE			DME TRANSMITTER SITE			ELEVATION ANTENNA SITE		
X	Y	Z	X	Y	Z	X	Y	Z
-1000.	-500.	5.	-5000.	-1000.	25.	-1000.	500.	5.
AIRCRAFT POSITION #26. OBSERVED DATA: RHO=32048.8 THETA=-21.90 PHI=5.15								
TRUE POS. INIT. EST.								
ITERATION NUMBER I	1	2	3	4	5	6		
X	25000.00	24736.02	24996.09	25000.04	25000.00	25000.00	25000.00	25000.00
Y	10000.00	11453.86	9999.59	10000.01	10000.00	10000.00	10000.00	10000.00
Z	2500.00	2882.00	2529.98	2499.90	2500.00	2500.00	2500.00	2500.00
AIRCRAFT POSITION #31. OBSERVED DATA: RHO=94342.5 THETA=-55.46 PHI=6.32								
TRUE POS. INIT. EST.								
ITERATION NUMBER I	1	2	3	4	5	6		
X	50000.00	48492.40	49963.61	50000.88	49999.97	49999.99	49999.99	49999.99
Y	75000.00	77211.41	74979.21	75000.48	74999.99	75000.00	75000.00	75000.00
Z	10000.00	10385.85	10110.61	9997.22	10000.06	10000.00	10000.00	10000.00
AIRCRAFT POSITION #36. OBSERVED DATA: RHO=94342.5 THETA=-55.46 PHI=6.32								
TRUE POS. INIT. EST.								
ITERATION NUMBER I	1	2	3	4	5	6		
X	50000.00	48492.40	49963.61	50000.88	49999.97	49999.99	49999.99	49999.99
Y	75000.00	77211.41	74979.21	75000.48	74999.99	75000.00	75000.00	75000.00
Z	10000.00	10385.85	10110.61	9997.22	10000.06	10000.00	10000.00	10000.00
AIRCRAFT POSITION #41. OBSERVED DATA: RHO=133060.1 THETA=-44.17 PHI=8.90								
TRUE POS. INIT. EST.								
ITERATION NUMBER I	1	2	3	4	5	6		
X	90000.00	90445.80	89914.30	90001.53	89999.96	90000.00	90000.00	90000.00
Y	90000.00	92209.77	89981.45	90000.59	89999.99	90000.00	90000.00	90000.00
Z	20000.00	20598.38	20298.63	19995.88	20000.13	20000.00	20000.00	20000.00
AIRCRAFT POSITION #46. OBSERVED DATA: RHO=107842.0 THETA=-29.02 PHI=1.10								
TRUE POS. INIT. EST.								
ITERATION NUMBER I	1	2	3	4	5	6		
X	90000.00	89300.65	89999.77	90000.00	90000.00	90000.00	90000.00	90000.00
Y	50000.00	51819.11	49999.93	50000.00	50000.00	50000.00	50000.00	50000.00
Z	2000.00	2081.47	2005.25	2000.00	2000.00	2000.00	2000.00	2000.00

Table D-1. Rotational Algorithm Exercise (continued)

GROUND STATION SITE GEOMETRY # 5								
AZIMUTH ANTENNA SITE			DME TRANSMITTER SITE			ELEVATION ANTENNA SITE		
X	Y	Z	X	Y	Z	X	Y	Z
-12000.	1000.	0.	-5000.	-1500.	5.	-1000.	-1000.	10.
AIRCRAFT POSITION #1. OBSERVED DATA: RHO=15531.3 THETA=-27.54 PHI=13.42								
TRUE POS. INIT. EST.								
ITERATION NUMBER I	1	2	3	4	5	6		
X	5000.00	8771.94	4918.00	4979.48	4999.90	5000.12	5000.00	5000.00
Y	10000.00	8180.09	10007.56	9991.47	9999.70	10000.04	10000.00	10000.00
Z	3000.00	3614.97	3504.63	3022.10	2997.29	2999.78	3000.01	3000.00
AIRCRAFT POSITION #6. OBSERVED DATA: RHO=10355.7 THETA=.00 PHI=8.90								
TRUE POS. INIT. EST.								
ITERATION NUMBER I	1	2	3	4	5	6		
X	5000.00	5355.68	4992.81	4999.93	5000.00	5000.00	5000.00	5000.00
Y	1000.00	1000.00	1000.00	1000.00	1000.00	1000.00	1000.00	1000.00
Z	1000.00	1611.50	1069.77	1000.69	1000.01	1000.00	1000.00	1000.00
AIRCRAFT POSITION #11. OBSERVED DATA: RHO=26518.1 THETA=-40.35 PHI=9.55								
TRUE POS. INIT. EST.								
ITERATION NUMBER I	1	2	3	4	5	6		
X	10000.00	15208.12	9957.43	9987.06	10000.01	10000.06	10000.00	10000.00
Y	20000.00	18170.96	20032.37	19991.28	19999.72	20000.04	20000.00	20000.00
Z	4000.00	4411.31	4424.53	4013.76	3998.13	3999.91	4000.01	4000.00
AIRCRAFT POSITION #16. OBSERVED DATA: RHO=16378.0 THETA=-10.29 PHI=4.52								
TRUE POS. INIT. EST.								
ITERATION NUMBER I	1	2	3	4	5	6		
X	10000.00	11114.39	9996.40	9999.85	10000.00	10000.00	10000.00	10000.00
Y	5000.00	3926.87	4999.94	4999.98	5000.00	5000.00	5000.00	5000.00
Z	1000.00	1300.02	1069.60	1000.20	999.99	1000.00	1000.00	1000.00
AIRCRAFT POSITION #21. OBSERVED DATA: RHO=51450.9 THETA=-46.25 PHI=5.87								
TRUE POS. INIT. EST.								
ITERATION NUMBER I	1	2	3	4	5	6		
X	25000.00	30579.96	24986.84	24997.14	25000.01	25000.00	25000.00	25000.00
Y	40000.00	38165.39	40022.38	39997.58	39999.96	40000.00	40000.00	40000.00
Z	5000.00	5270.56	5251.12	5003.90	4999.68	4999.99	5000.00	5000.00

Table D-1. Rotational Algorithm Exercise (concluded)

GROUND STATION SITE GEOMETRY # 5

AZIMUTH ANTENNA SITE			DME TRANSMITTER SITE			ELEVATION ANTENNA SITE		
X	Y	Z	X	Y	Z	X	Y	Z
-12000.	1000.	0.	-5000.	-1500.	5.	-1000.	-1000.	10.

AIRCRAFT POSITION #26. OBSERVED DATA: RHO=32225.4 THETA=-13.64 PHI=5.04
TRUE POS. INIT. EST.

ITERATION NUMBER I	1	2	3	4	5	6
X	25000.00	26316.33	24995.62	24999.80	25000.00	25000.00
Y	10000.00	8600.16	10000.34	9999.96	10000.00	10000.00
Z	2500.00	2841.30	2584.47	2500.32	2499.99	2500.00

AIRCRAFT POSITION #31. OBSERVED DATA: RHO=94747.8 THETA=-49.68 PHI=6.23
TRUE POS. INIT. EST.

ITERATION NUMBER I	1	2	3	4	5	6
X	50000.00	56307.31	49981.52	49997.39	50000.01	50000.00
Y	75000.00	73239.63	75033.71	74997.97	74999.95	75000.00
Z	10000.00	10290.61	10290.06	10005.37	9999.72	9999.99

AIRCRAFT POSITION #36. OBSERVED DATA: RHO=94747.8 THETA=-49.68 PHI=6.23
TRUE POS. INIT. EST.

ITERATION NUMBER I	1	2	3	4	5	6
X	50000.00	56307.31	49981.52	49997.39	50000.01	50000.00
Y	75000.00	73239.63	75033.71	74997.97	74999.95	75000.00
Z	10000.00	10290.61	10290.06	10005.37	9999.72	9999.99

AIRCRAFT POSITION #41. OBSERVED DATA: RHO=133405.6 THETA=-40.57 PHI=8.83
TRUE POS. INIT. EST.

ITERATION NUMBER I	1	2	3	4	5	6
X	90000.00	96334.04	89945.45	89995.49	90000.04	89999.99
Y	90000.00	87766.70	90038.56	89997.91	89999.95	90000.00
Z	20000.00	20486.39	20505.90	20010.35	19999.54	19999.99

AIRCRAFT POSITION #46. OBSERVED DATA: RHO=108079.7 THETA=-25.65 PHI=1.09
TRUE POS. INIT. EST.

ITERATION NUMBER I	1	2	3	4	5	6
X	90000.00	92424.98	89999.90	89999.99	90000.01	90000.01
Y	50000.00	47793.20	50000.17	50000.00	50000.00	50000.00
Z	2000.00	2071.41	2023.43	2000.01	2000.00	2000.00